Ionoelastomers at Electrified Interfaces:

Differential Electric Double Layer Capacitances of Crosslinked Polymeric Ions and Mobile Counter

Heewoon Shin¹, Jowon Shin¹, Ryan C. Hayward² and Hyeong Jun Kim¹,*

Ions

¹ Department of Chemical and Biomolecular Engineering, Sogang University, Seoul, 04107, Korea

² Department of Chemical and Biological Engineering, University of Colorado, Boulder, Colorado 80303, USA

KEYWORDS Ionoelastomer, Electric Double Layer Capacitance, Crosslinked Polymerized Ionic Liquids,

ABSTRACT

Ionoelastomers (IEs), consisting solely of crosslinked networks of polymerized ionic liquids (PILs), have gained attention for use in various electrochemical applications due to their unique combination of the electrochemical properties of ionic liquids (ILs) and the solid-state elastic properties of the polymer networks. However, the structure of the electric double layer (EDL) of IEs at electrified surfaces is not well understood, especially when considering that one of the ionic species is covalently bound to the crosslinked polymer network. Herein, we investigate the differential EDL capacitances of crosslinked polymeric ions and counter ions in IEs. A pair of IEs with opposite polarity is prepared; the polycationic IE with crosslinked imidazolium cations and free bis(trifluoromethyl sulfonyl)imide (TFSI-) anions and the polyanionic IE with crosslinked sulfonimide anions and free 1-ethyl-3-methylimidazolium (EMIM⁺) cations. By applying two electrodes with a large contrast in surface area, the EDL capacitances of the crosslinked polymeric ions and the mobile counter ions can be decoupled. We find that the EDL capacitances of the fixed ions are lower than that of the counter ions in both the polyanion and polycation IEs, resulting in a highly asymmetric capacitance response depending on the sign of the applied voltage. Without crosslinking, we observe similar EDL capacitances for polymeric ions and counter ions, suggesting that the elastic energy of the crosslinked networks in IEs restricts the freedom of polymeric ions to rearrange at the electrified surfaces, thereby reducing the EDL capacitance.

Introduction

Ionoelastomers (IEs) are an emerging class of materials where one ionic species of an ionic liquid (IL) is tethered to an elastomeric polymer network, while the counterion is mobile. 1-6 These materials have gained attention due to their combination of the electrochemical properties of ILs and the solid-state properties of elastomeric polymers, making them attractive for use in a variety of electrochemical applications.^{7,8} Examples of demonstrated devices include electrolytes for supercapacitors^{9,10} and batteries, ^{11–13} exchange membranes in fuel cells, ¹⁴ gating materials in field-effect transistors, ¹⁵ electro-active actuators,³ and osmotic energy conversions.^{16,17} Additionally, IEs have been shown to be soft ionic analogs of p-type and n-type semiconductors since the covalent bonding of one species of ions to the crosslinked networks permits selective conduction of free counter ions.^{2,6,18} Coupled with their soft, elastic, and liquid-free nature, IEs offer great potential in the newly emerging field of "ionotronics" in which device functions rely on ions as charge carriers. 1,19-21 The polyanion/polycation junction of IEs enables the design of ionotronic devices such as ionic diodes, ^{6,9,22} transistors, ^{18,23} electro-adhesives, ^{4,24} and electro-mechanical transducers² with high deformability, optical transparency, bio-compatibility, and softness of which those properties are not easily accessible in conventional electronic devices. 3,4,6,22-26

The formation of an electric double layer (EDL) is a universal feature of ionic materials at the electrified interfaces, and the ion distribution in the EDL significantly impacts various electrochemical properties such as capacitance, redox reactions, charging/discharging rates, and electric field strength.^{27–33} As the driving force behind electrochemical reactions relies on the voltage difference between the electrode and the reactants, even small changes in the EDL voltage can lead to variations in electrochemical reaction currents by orders of magnitude.^{31,34} Therefore, understanding the EDL structure and its dependence on the electrode potential is of

great importance for the performance of IEs in various electrochemical applications. In diluted electrolytes, the classical Gouy-Chapman-Stern (GCS) theory describes the Debye length (ξ) as becoming exponentially small with increasing electrode polarization, resulting in a U-shaped differential capacitance curve as a function of voltage.^{29,30,34} For highly concentrated electrolytes, such as ILs, the effects of finite ion size and excluded volume become significant. The modified mean-field model that accounts for the finite size of ions explains that as the voltage increases, the ions in ILs will start to line up in front of the electrode, causing the EDL to become thicker and the capacitance to decrease. As a result, the shape of the capacitance curve falls in either a "bell" or "camel" shape depending on the compactivity parameter of the IL.^{30,33,35} This model has been supported by numerous simulation results and experimental studies that have observed bell and camel-shaped capacitance curves for various ion sizes³⁶, types of electrodes,^{37,38} temperatures^{39,40}, and solvent dilution effects of ILs.⁴¹

Despite the success of describing the EDL structure of various ionic materials, the covalent bonding of one ionic species to polymeric backbones or crosslinked networks introduces new considerations. The EDL structure of polymerized ionic liquids (PILs) has been studied using the polyelectrolyte adsorption model and molecular dynamics (MD) simulations, which predict higher EDL capacitances of polymeric ions due to the surface absorption of charged polymer chains upon applying an electric potential. PlLs on a charged electrode a self-consistent field theory for the local electrostatic potential of PILs on a charged electrode. Their finding suggests that the differential capacitance profile is strongly sensitive to the boundary condition for the local polymer concentration on the electrode. When there is a short-range depletion of the polymer ions near the charged surfaces, the differential capacitance shows a camel-shaped curve with two strongly asymmetric peaks and significantly decreased capacitance from the polymeric ions. Experimentally, Kumar et al. Pexplored the EDL structures of PILs at electrified interfaces using broadband dielectric spectroscopy. In

their experiments, capacitance-voltage response curves were qualitatively similar to the corresponding ILs, suggesting that covalent linking of one ionic species of ILs to the polymeric backbones does not significantly influence the EDL structures in close proximity to electrode surfaces. However, in contrast to PILs, the movement of polymeric ions in IEs toward the electrified surfaces can be significantly impeded by the elastic deformation of the networks. To the best of our knowledge, the elastic energy associated with polyelectrolyte networks has not yet been considered in describing the EDL, where the long-range motion of the crosslinked polymeric ions in IEs requires elastic deformation of the network.

In this study, we investigate the differential EDL capacitance responses of IEs at electrified surfaces. Specifically, the differential EDL capacitances of crosslinked polymeric ions and free counter ions are experimentally measured. We prepare two oppositely charged pairs of IEs with nearly symmetric chemical functionalities. The polycation IE is composed of fixed imidazolium cations and free bis(trifluoromethyl sulfonyl)imide (TFSI-) anions, while the polyanion IE is composed of fixed trifluoromethane sulfonimide anions and free 1-ethyl-3methylimidazolium (EMIM⁺) cations. To decouple the differential EDL capacitance of crosslinked polymer ions and free ions formed at the electrified interfaces, we apply two electrode configurations with a large difference in the surface areas, which allows us to eliminate the contribution of the EDL capacitance at the high surface area electrode due to its negligible contribution to the overall capacitance. Our experimental results show highly asymmetric camel shape capacitance responses with the EDL capacitance of crosslinked polymeric ionic species being lower than that of free ionic species in both polyanion and polycation IEs. The asymmetries are attributed to the restricted degree of freedom of the crosslinked polymeric ions, which constrains the closer packing of ions toward to the electrified interfaces. With the increase in crosslinking density of IEs, a greater reduction in EDL capacitance is observed, along with an amplified asymmetry between crosslinked polymeric ions and free ions. Moreover, without crosslinking, we observe similar EDL capacitances for polymeric ions and counter ions, supporting that the elastic energy of crosslinked networks in IEs reduces differential EDL capacitances of crosslinked ions. Our finding suggests that the elastic energy of the networks has to be accounted for in describing the EDL structures of IEs and their use in other electrochemical applications.

RESULTS AND DISCUSSION

Figure 1. Chemical structures of polycation AT and polyanion EA monomers. Polymerization of each monomer with the crosslinker forms a pair of oppositely charged polycation (PAT) and polyanion (PEA) IEs.

A pair of oppositely charged IEs is prepared based on the chemical structures of 1ethyl-3-methylimidazolium bis(trifluoromethyl sulfonyl)imide (EMIM TFSI) IL. EMIM TFSI is one of the most widely used ILs in many electrochemical applications due to its hydrophobicity, high ionic conductivity, and excellent electrochemical stability. 45–47 One of the ionic charges in the EMIM TFSI IL is functionalized with polymerizable acrylate groups following modified literature procedures.^{2,4,48} The resulting polycation and polyanion monomers are 1-[2-acryloyloxyethyl]-3-butylimidazolium bis(trifluoromethane) sulfonimide (AT) and 1-ethyl-3methyl imidazolium 3-[[[(trifluoromethyl) sulfonyl]amino] sulfonyl]propyl acrylate (EA), respectively (Scheme 1). The detailed synthetic procedures are described in the Supporting Information including a modified method for preparing the EA monomer based on a sulfur-fluoride exchange (SuFEx) reaction. 49,50 The synthesis of AT and EA monomers is confirmed by ¹H-NMR and ¹⁹F-NMR spectroscopy (Figures S1-S2). The free-radical polymerization of AT and EA monomers with 2 mol% poly (ethylene glycol) diacrylate (PEGDA) crosslinkers yields transparent, soft, and highly-stretchable polycationic (PAT) and polyanionic (PEA) IEs, respectively. Both PAT and PEA IEs present rubbery solid-like characteristics, showing a larger storage modulus (G') than loss modulus (G") under the dynamic shear deformation at ambient temperature (HR20, TA instruments) (Figure S3). The G' values of PAT and PEA with 2 mol% of crosslinking were found to be 0.19 MPa and 0.11 MPa, respectively. As decreasing temperatures, PAT and PEA undergo glass transitions at -3 °C and -9 °C, respectively, resulting in almost four orders of magnitude increase in G' and G' with the distinctive peak of tan δ ($\delta = G'/G''$). The glass transition temperatures ($T_g s$) of both IEs are far lower than room temperature, enabling ion conduction under ambient conditions in both PAT and PEA IEs through chain segmental relaxations. Under the static linear deformation, the elastic modulus of PAT and PEA were measured to be 0.5 and 0.4 MPa, respectively (**Figure S4**), comparable to previously reported values for similar IEs.^{2,4,6} Detailed experimental procedures and characterization of IEs are described in the Supporting Information.

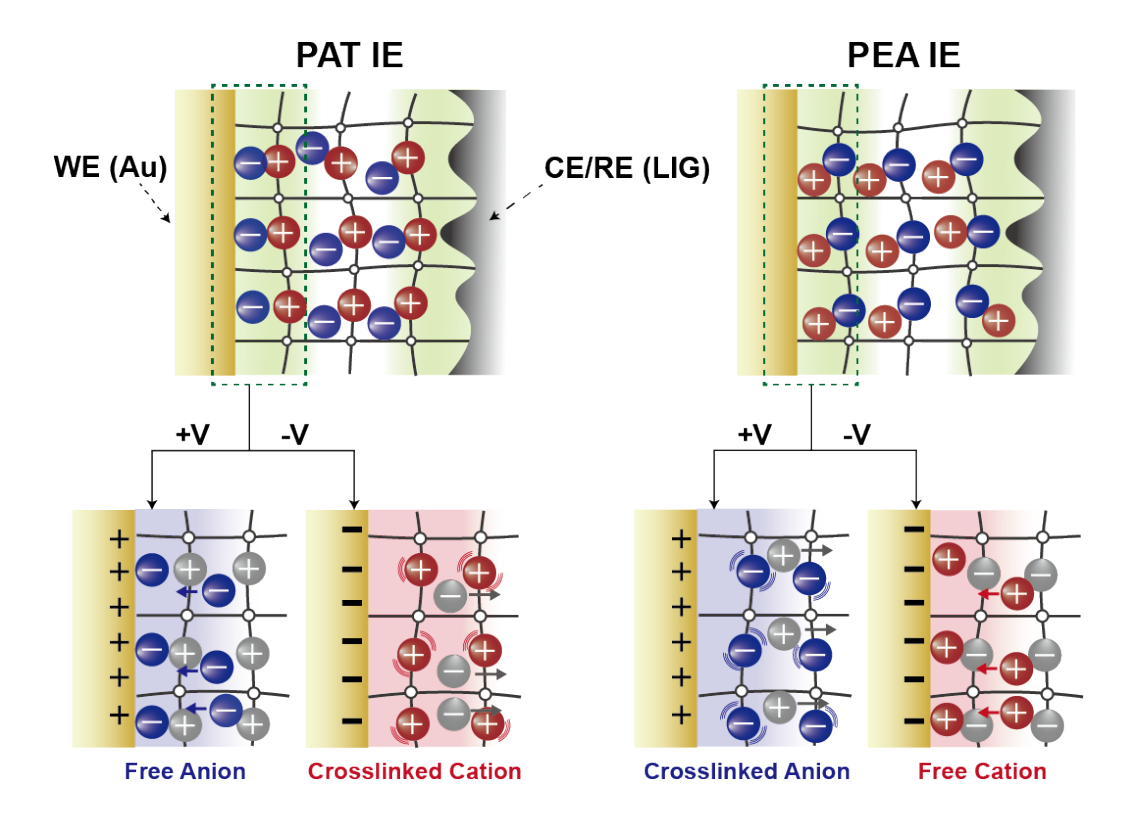


Figure 2. The illustration of two-electrode geometry with large surface area asymmetry, designed to separate the EDL capacitances of crosslinked polymeric ions and free counter ions. When a positive potential is applied to the WE for PAT polycation IEs, an EDL consisting of free ions forms. In contrast, applying a negative potential to the WE results in an EDL composed of crosslinked polymeric ions. The opposite behavior occurs for PEA polyanion IEs.

To investigate the decoupled differential EDL capacitances of crosslinked polymeric ions and counter ions in PEA and PAT IEs, we employ a two-electrode system with a large asymmetry in surface area between the working electrode (WE) and counter/reference electrode (CE/RE). Since the two EDL capacitors formed at the WE and CE/RE are connected in series, the reciprocal of the total capacitance ($1/C_{total}$) is equal to the sum of the reciprocals of the two capacitors. We apply microporous laser-induced graphene (LIG) electrode^{51–53} as a

CE/RE, while a flat Au serves as the WE. Due to the exfoliated micro-porous structure of LIG, it provides a much larger surface area than the flat electrodes, resulting in considerably higher EDL capacitances at CE/RE compared to WE. Consequently, the contribution of the reciprocal EDL capacitance at the CE/RE can be almost ignored in relation to the total capacitance (1/C_{total} = $1/C_{WE} + 1/C_{CE/RE} \approx 1/C_{WE}$). Therefore, the decoupled EDL capacitance of either polymeric or counter ions can be measured depending on the polarity of the WE (Figure 2). For experimental demonstrations, we prepared a 1 cm² square-patterned LIG by engraving the surface of a polyimide substrate with CO₂ laser (VLS2.30DT, ULS) (Figure S5). The prepared LIG electrode was placed between two fluorinated glass slides separated by 300 µm polyimide spacers. Then, the AT or EA monomer solution with 2 mol% PEGDA crosslinkers was injected into the mold. Free-radical polymerization was conducted by exposure of a photoinitiator (2,2dimethoxy-2-phenylacetophenone, DMPA) to 365 nm UV light. As a result, microporous LIG can be embedded on one side of the IE. Subsequently, a thermally deposited flat Au electrode (~ 50 nm thick) on a glass substrate was attached to the top of the IEs to achieve an Au/LIG electrode geometry (Scheme S1). For control samples, PAT and PEA with symmetric WE and CE/RE electrodes (i.e., Au/Au and LIG/LIG) were also prepared. For the Au/Au symmetric electrode system, two Au electrodes on glass substrates are attached on top and bottom of bare IEs with a thickness of 300 μm. In the case of the symmetric LIG/LIG geometry, two bare surfaces of LIG-embedded IEs each with a thickness of 150 µm, are attached together.

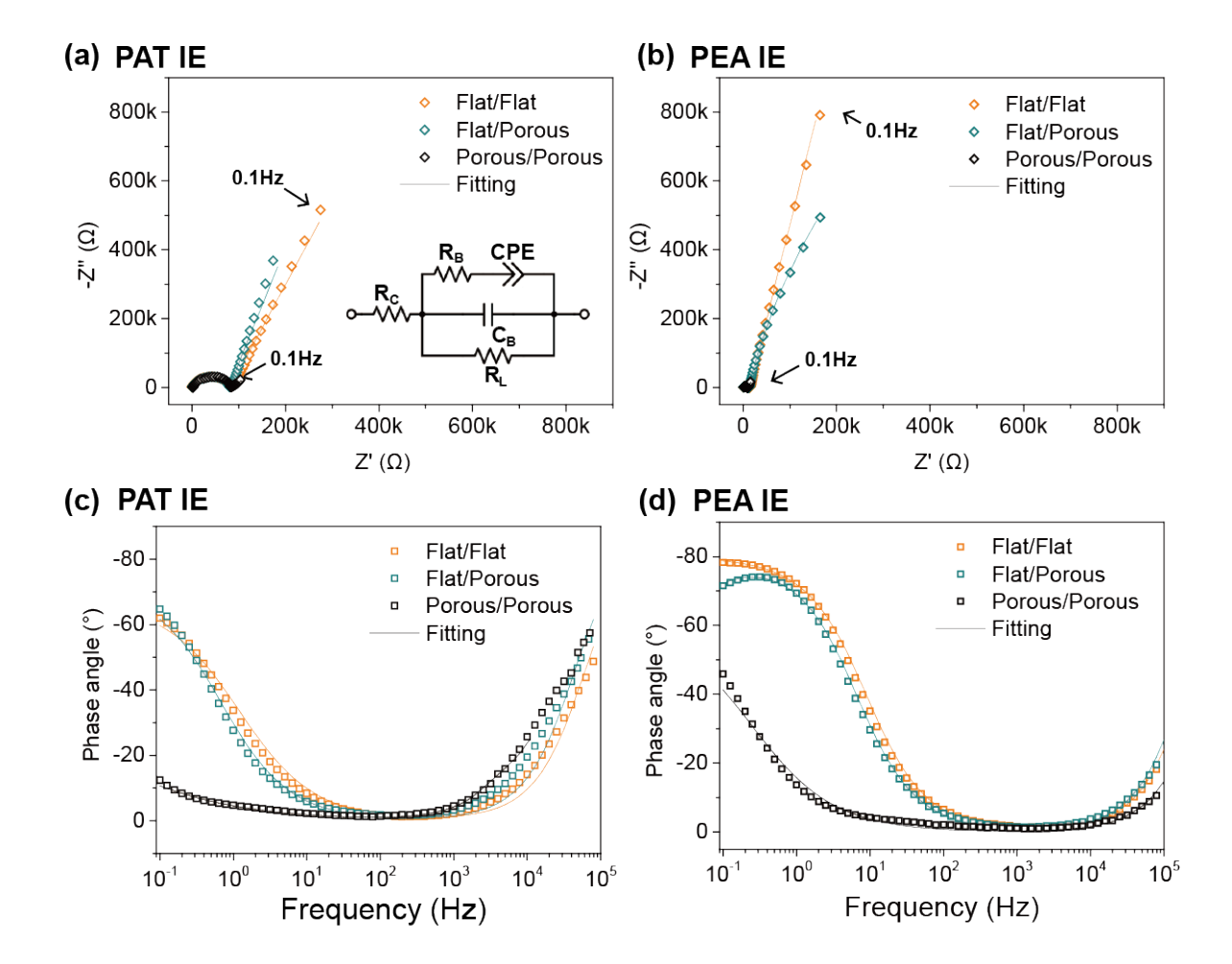


Figure 3. (a), (b) Nyquist plots (Z' vs Z') and (c), (d) Bode phase plots (phase angle vs frequency) of AC-impedance are presented for PAT polycation and PEA polyanion IEs with LIG/LIG, Au/Au, and Au/LIG electrode configurations. The solid lines in the plots represent the fits obtained from the equivalent circuit model depicted in the inset of (a) to the AC-impedance data.

Table 1. Fitting parameters of electrochemical impedance spectroscopy (EIS) measurement.

Polymer	Type	$R_{B}\left(k\Omega\right)$	СРЕ			EDL	Conductivity ^{a)}
			$Q_{\alpha} \times 10^{-6}$	α	$C_{B}(pF)$	capacitance ^{a)} $(\mu F/cm^2)$	$(\times 10^{-4} \mathrm{mS/cm^2})$
PAT IE (Polycation)	Au/Au	80.3 ± 0.9	2.76 ± 0.09	0.75 ± 0.01	42 ± 1	1.2 ± 0.2	3.7 ± 0.1
	LIG/LIG	80.5 ± 0.3	37.6 ± 0.4	0.40 ± 0.01	112 ± 2	200 ± 10	3.6 ± 0.2
	Au/LIG	78.2 ± 0.7	4.01 ± 0.08	0.81 ± 0.01	61 ± 1	3.0 ± 0.2	4.2 ± 0.1
PEA IE (Polyanion)	Au/Au	14.7 ± 0.1	1.91 ± 0.01	0.88 ± 0.01	47 ± 2	1.3 ± 0.4	16 ± 1
	LIG/LIG	9.4 ± 0.5	82.1 ± 0.5	0.70 ± 0.02	273 ± 1	80 ± 5	32 ± 1
	Au/LIG	14.1 ± 0.1	4.37 ± 0.03	0.90 ± 0.01	52 ± 2	3.2 ± 0.2	22 ± 1

a) Average from a minimum of 10 measurements for each of 5 different samples

AC-impedance responses of PEA and PAT IEs are characterized using electrochemical impedance spectroscopy (EIS) (Reference 620, Gamry Instruments) over a frequency range of 0.1 Hz to 1 MHz with an AC amplitude of 40 mV. The Nyquist (Z' vs Z") and Bode phase angle (phase angle vs frequency) plots of the AC-impedance response of PAT and PEA IEs are shown in Figure 3. The Nyquist plots for each IE show two distinct regions: a semicircle at higher frequencies $(10^3 - 10^6 \text{ Hz})$ and a tilted straight line at lower frequencies $(0.1 - 10^3 \text{ Hz})$, consistent with the previously reported AC-impedance response of IEs.^{2,4} The semicircle at high frequencies corresponds to the response of bulk polarization (C_B in the equivalent circuit model) and bulk resistance (R_B) from ion conduction, while the tilted straight line at low frequencies is a result of the accumulation of ions at the interface during the formation of EDL capacitors (constant phase element, CPE). At high frequencies, the rapid alternation of voltage signs induces bulk polarization, resulting in a capacitor-like behavior with a phase angle close to 90 degrees in Bode phase angle plots. At moderate frequencies, bulk transport of ions takes place, resulting in a resistor-like behavior with a phase angle close to 0 degrees, and finally at the lowest frequencies, ion accumulation leads to the formation of EDL capacitors with increased phase angle. Following the previous literature,² all impedance curves are fitted (ZView, Scribner Associates) based on the equivalent circuit model of IEs, as shown in the insets of Figure 3(a). Fitted parameters for PAT and PEA IEs are summarized in Table 1.

Based on the fitting parameters, two important variables—ion conductivity and frequency-independent EDL capacitances—can be derived. The ion conductivity of PEA and PAT IEs can be calculated from the R_B of fitting parameters (**Table 1**). Ion conductivities for PAT and PEA IEs with symmetric Au/Au electrodes are measured to be $(3.7 \pm 0.1) \times 10^{-4}$ mS/cm and $(1.6 \pm 0.1) \times 10^{-3}$ mS/cm, respectively, which are in reasonable agreement with previous reports on ion conductivity of IEs.^{2,6,54} The higher ion conductivity of PEA is likely due to its lower T_g . As expected, similar ion conductivities are measured regardless of the

electrode configurations whether symmetric (Au/Au, LIG/LIG) or asymmetric (Au/LIG) electrodes are used. However, in stark contrast, the EDL capacitance of PEA and PAT strongly depends on the electrode configurations. A frequency-independent EDL capacitance can be extracted from the characteristics of the constant phase element (CPE) used in the equivalent circuit following relation: $C_{EDL} = Q_{\alpha}^{1/\alpha} R_{\Omega}^{[(1/\alpha)-1]}$ where R_{Ω} represents the resistive limit of the CPE, herein $R_{\Omega} = R_B$, and Q_{α} and α are constants for describing impedance of CPE ($Z_{CPE} = Q_{\alpha}^{-1}$ $^{1}(j\omega)^{-\alpha}$, $0 \le \alpha \le 1$). 55-56 The PAT with microporous LIG/LIG electrodes exhibits an EDL capacitance of $170 \pm 10 \, \mu F/cm^2$, which is more than 100 times greater than that of planar Au/Au electrodes $(1.2 \pm 0.2 \mu F/cm^2)$. As a result, at the same frequency of 0.1 Hz, the reactance (Z") and phase angles of PAT with microporous LIG/LIG electrodes are much smaller compared to those with the planar Au/Au electrodes (Figure 3). Interestingly, the EDL capacitance of PAT with the asymmetric pair of Au/LIG electrodes is measured to be 3.4 ± 0.2 μF/cm². Given the large surface area of the LIG, this interface should contribute negligibly to the total capacitance, and thus we would expect roughly twice the capacitance value than that measured for the planar Au/Au electrode. For polyanion PEA IEs, a similar behavior is observed, with the capacitance of $3.2 \pm 0.2 \,\mu\text{F/cm}^2$ with Au/LIG asymmetric electrodes being roughly twice that of the planar Au/Au electrodes (1.5 \pm 0.4 μ F/cm²). Therefore, we conclude that the EDL capacitance at the single planar Au electrode can be successfully isolated using the Au/LIG asymmetric electrode geometry, and we apply this principle as follows to decouple the differential EDL capacitance of crosslinked polymeric ions and free counter ions in IEs.

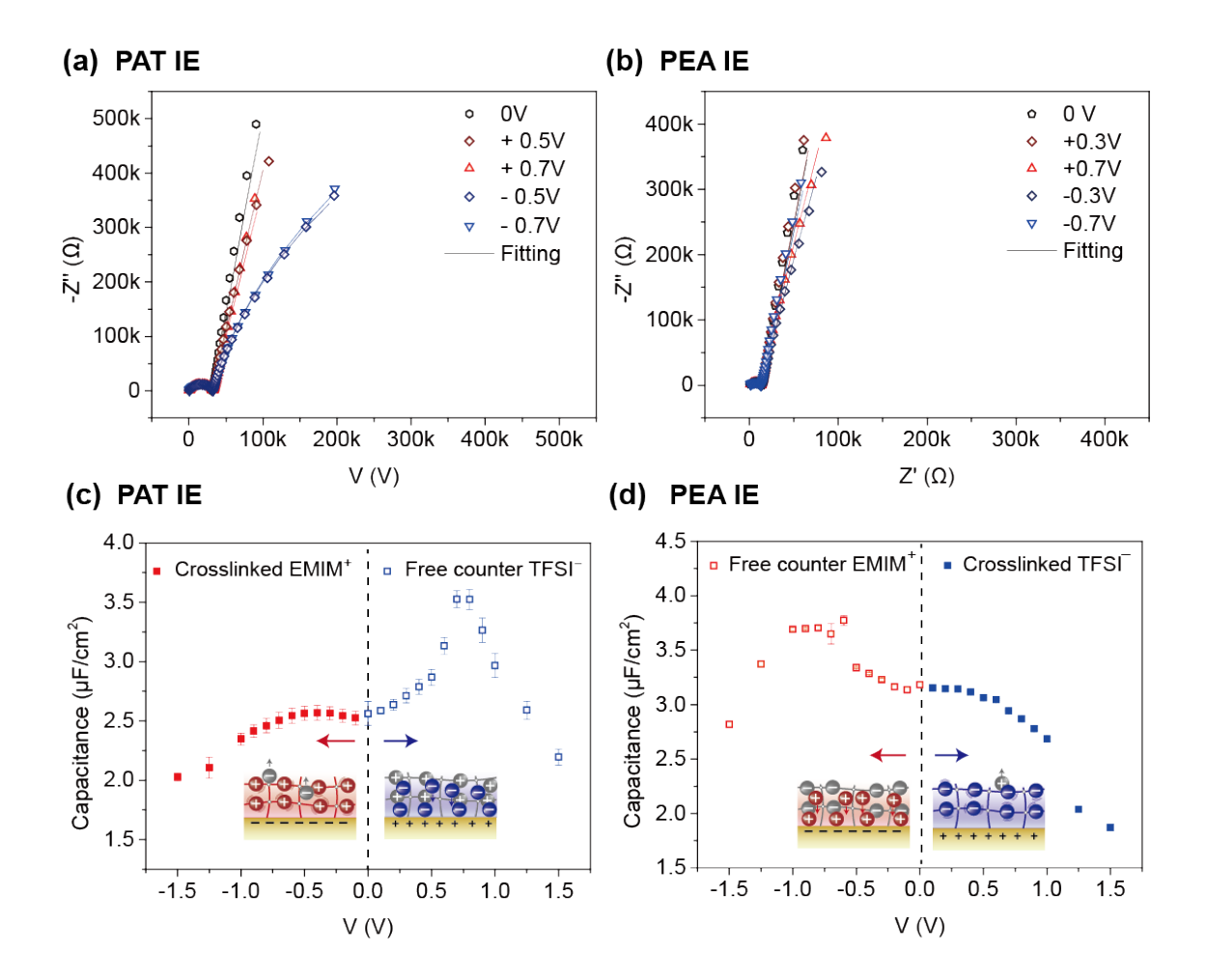


Figure 4. Nyquist plots from AC-impedance measurement of (a) polycation PAT and (b) polyanion PEA IEs with Au/LIG electrode geometry under various DC biases. Solid lines represent fits of the equivalent circuit model. The frequency-independent EDL capacitances for (c) polycation PAT and (d) polyanion PEA are plotted as a function of applied DC voltage. Highly asymmetric camel shape capacitance responses are observed with reduced EDL capacitances from crosslinked polymeric ions in both PAT and PET IEs.

Decoupled differential EDL capacitances of polymeric ions and counter ions are characterized by the EIS while applying constant DC biases to the WE (Au) and CE/RE (LIG). The Nyquist plots of AC-impedance measurements for PAT and PEA IEs under various DC biases are shown in **Figure 4(a)** and **Figure 4(b)**, respectively. Each curve from PAT and PEA IEs is fitted with the equivalent circuit model, and calculated frequency-independent EDL

capacitances are plotted as a function of applied potential in Figure 4(c) and Figure 4(d). Full data is shown in the Supporting Information (Table S1). We note that the applied DC potential of \pm 1.5 V lies within the electrochemical window of PAT and PEA with Au/Au and LIG/LIG electrodes (Figure S6), indicating that the current detected through EIS in our experiments primarily originates from non-Faradaic processes. Both PAT and PEA IEs show a typical camel-shaped response of capacitance-voltage curves with increasing electrode polarization. However, the capacitance responses of both PAT and PEA are highly asymmetric depending on the sign of the applied voltage. For example, when a positive bias of 0.7 V is applied to PAT, free TFSI counter ions align at the positively charged WE, resulting in an increase of EDL capacitances from 2.53 μF/cm² to 3.58 μF/cm². On the other hand, when a negative bias is applied, TFSI counter ions drift away from the negatively charged WE, and imidazolium polymeric cations attached to the crosslinked networks form an EDL. Interestingly, the increase in EDL capacitance is less pronounced than that of the free counter ions, yielding a highly asymmetric camel-like response. The maximum EDL capacitance of crosslinked polymeric ion was measured to be 2.57 μF/cm² at a voltage of -0.5 V. In the case of the polyanion PEA IE, opposite capacitance-voltage responses to those of polycation PAT IE are observed. Under a positive bias, free EMIM⁺ ions form an EDL, resulting in increased capacitance while crosslinked polymeric sulfonimide anions ions maintain similar capacitance values under a negative bias. The notably smaller EDL capacitances from the crosslinked polymeric ions in both PEA and PAT IEs imply that the restricted movement of the crosslinked ions toward the electrified electrodes contributes to a reduction in the differential EDL capacitances.

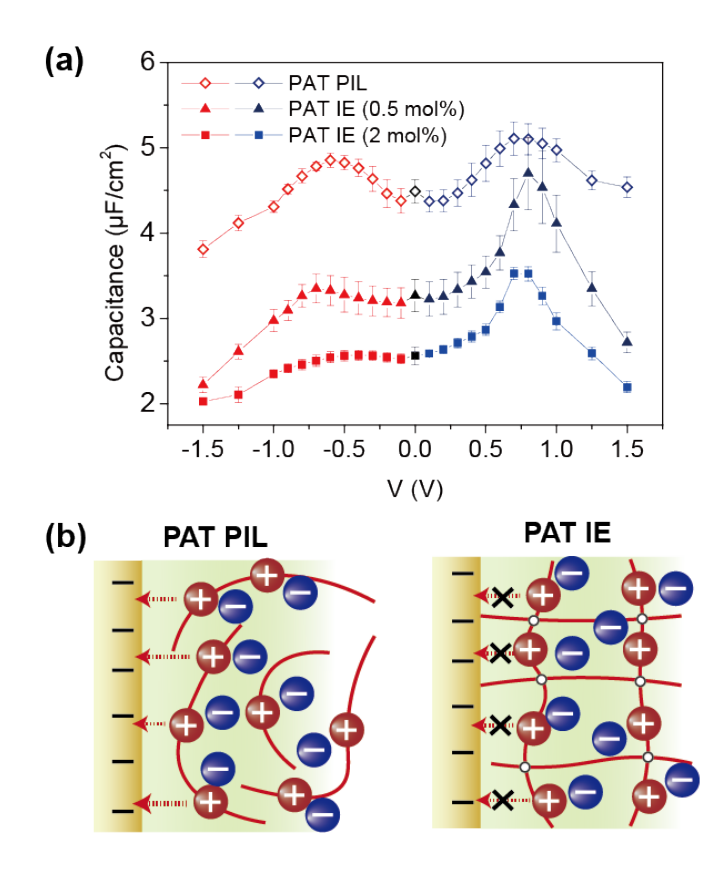


Figure 5. (a) Differential EDL capacitance responses of polycation PAT PIL without crosslinking and PAT IEs with crosslinking densities of 0.5 mol% and 2 mol%. (b) Schematic illustration of PIL and IE at the electrified interfaces.

To gain a deeper understanding of the effect of network elasticities on the EDL capacitances, we compared the capacitance responses of polycation PAT IEs with different crosslinking densities (0.5 mol% and 2 mol%) and polycation PAT PIL without crosslinking. The EDL capacitance responses of polycation PAT PIL and PAT IEs are compared in **Figure 5(a)** and full data is shown in the Supporting Information (**Figure S7-S8, Table S2**). The PAT PIL was prepared using the same procedure as for the PAT IE, except that PEGDA crosslinkers were excluded. The viscosity of PAT PIL is measured to be 82.2 kPa·s with a G' of 33.4kPa and G" of 75.1 kPa at 1.0 rad/s under dynamic shear deformation. The G" of PAT PILs is higher than the G' in an angular frequency range of 0.1-100 rad/s, revealing the liquid-like behavior

of the PILs (Figure S9). In contrast, the PAT IEs with 0.5 mol% and 2 mol% crosslinking density show an G' of 86 kPa, and 120 kPa at 1.0 rad/s, respectively, with G' exceeds G" over the whole frequency range, indicative of the solid-like behavior of the IEs (**Figure S9**). The same Au/LIG electrode geometry is applied to decouple EDL capacitance between polymeric ions and free counter ions for PILs and IEs. When the IEs are not crosslinked, we observe similar EDL capacitances for polymeric ions and counter ions without significant asymmetry in the response shape. Upon applying positive biases to PAT PILs, TFSI counter ions drift and align at the electrode, resulting in an increase of EDL capacitances from 4.4 ± 0.1 at 0 V to 5.1 \pm 0.2 μ F/cm² at 0.7 V. Conversely, under negative bias, the accumulation of imidazolium polymeric cations to the electrode also causes an increase of EDL capacitance with a maximum peak of $4.9 \pm 0.1 \,\mu\text{F/cm}^2$ at - 0.6 V, exhibiting a similar response to that of free counterions. Similar symmetric EDL capacitance-voltage responses of PILs with the reversal of voltage were also experimentally observed by Kumar et al.²⁷ The shape of the capacitance-voltage curve of PIL is qualitatively similar to that of the IL despite the chain connectivity of the polymeric ions. As adding a crosslinker (0.5 mol% and 2 mol%) to form a crosslinked network of PAT PILs, an asymmetry between polymeric ions and free counter ions starts to appear. The crosslinking of PILs reduces overall differential EDL capacitance but the decrease in EDL capacitances of free counter ions is less pronounced than that of crosslinked polymeric ions, leading to highly asymmetric voltage-capacitance responses in IEs. As more crosslinkers are added, a further reduction in capacitance is observed, providing experimental evidence that crosslinked networks of polymeric ions in the IEs reduce the EDL capacitances.

In the absence of crosslinking, when a negative voltage is applied to the polycation PIL, free anions move away from the WE, while polymeric cations can also drift toward the WE (**Figure 5(b)**). Consequently, polymeric ions and free counter ions can be aligned similarly in close proximity to the electrode surfaces, resulting in the symmetrical camel-like response of

EDL capacitances. However, once all the polymeric ions are crosslinked by the network, the drift of polymeric ions requires elastic energy of deformation. Due to this energy penalty, the separation distance in the EDL can be limited for crosslinked polymeric ions compared to free counter ions. Thus, an asymmetric camel-shaped capacitance-voltage response is observed for IEs. A recent theoretical study by Budkov et al. 44 also predicted an asymmetric camel-shaped curve in PILs with a significant reduction in the capacitance of the polymeric ions when there is a short-range depletion of polymeric ions near the charged surfaces. Since the network elasticity and crosslinking in the IE restrict the ability of network strands to adsorb to the electrified interface relative to a PIL, similar asymmetric capacitance responses with reduced capacitances from polymeric ions can be obtained from IEs. Therefore, our finding suggests that a revised framework is necessary to properly describe the ion distribution in EDL of IEs, accounting for the effect of elastic energy of the networks and its impact on electrochemical properties.

CONCLUSIONS

In conclusion, we examine the differential EDL capacitance response of IEs at electrified interfaces. Especially, our work provides experimental evidence of EDL capacitance differences between crosslinked polymeric ions and counter ions in the IEs. Two oppositely charged symmetric pairs of IEs based on EMIM TFSI ILs are prepared, where the polycation PAT is composed of fixed imidazolium cations and free TFSI anions, while the polyanion PEA is composed of fixed sulfonimide anions and free EMIM+ cations. To separate EDL capacitances of crosslinked polymer ions and counter ions, we apply asymmetric LIG/Au electrodes that exhibit a large difference in surface area. Due to the negligible contribution to the overall capacitances from the large surface area of LIG electrode, the decoupled EDL capacitance of either crosslinked polymeric or counter ions only at the flat Au electrode can be measured, depending on the polarity of the WE. We analyze the differential EDL capacitance

behavior of oppositely charged IEs using EIS while applying various DC biases and observe highly asymmetric voltage responses depending on the sign of the applied voltage. For both polyanion and polycation, the EDL capacitance of crosslinked polymeric ions is lower than that of the counter ions. Higher crosslinking density induces lower capacitances of polymeric ions, suggesting that the elastic networks restrict the degree of freedom of crosslinked ions, leading to lower EDL capacitances. Our work provides experimental evidence of differential EDL capacitances between crosslinked polymeric ions and counter ions for a better understanding of the EDL structures of IEs at the electrified interfaces, which is of great importance for the performance of IEs in various electrochemical applications.

ASSOCIATED CONTENT

Supporting Information. Detailed experimental procedure and additional characterization data. This material is available free of charge *via* the Internet at http://pubs.acs.org

Detailed experimental procedures and additional characterization (PDF)

AUTHOR INFORMATION

Corresponding Author

Hyeong Jun Kim* - Department of Chemical and Biomolecular Engineering, Sogang University, Seoul, 04107, Korea

Authors

Heewoon Shin - Department of Chemical and Biomolecular Engineering, Sogang University, Seoul, 04107, Korea

Jowon Shin - Department of Chemical and Biomolecular Engineering, Sogang University, Seoul, 04107, Korea

Ryan C. Hayward - Department of Chemical and Biological Engineering, University of Colorado, Boulder, Colorado 80303, USA

Author Contributions

H. J. Kim and **R.C. Hayward** supervised the project. **H. Shin** designed the experiments, solved the technical issues, and checked the experimental results. **J. Shin** contributed to the analysis of the rheological properties and discussion of the data. All authors contributed to developing the concept, interpreting the results, and preparing the manuscript.

ACKNOWLEDGMENT

This research was supported by the National Research Foundation of Korea (NRF-2022R1C1C1013490) and C1 Gas Refinery Program through the NRF funded by the Ministry of Science and ICT (2015M3D3A1A01064929).

REFERENCES

- (1) Park, J.-M.; Lim, S.; Sun, J.-Y. Materials Development in Stretchable Iontronics. *Soft Matter* **2022**, *18* (35), 6487–6510.
- (2) Kim, H. J.; Chen, B.; Suo, Z.; Hayward, R. C. Ionoelastomer Junctions between Polymer Networks of Fixed Anions and Cations. *Science* **2020**, *367* (6479), 773–776.
- (3) Ming, X.; Zhang, C.; Cai, J.; Zhu, H.; Zhang, Q.; Zhu, S. Highly Transparent, Stretchable, and Conducting Ionoelastomers Based on Poly (Ionic Liquid) s. *ACS Appl. Mater. Interfaces* **2021**, *13* (26), 31102–31110.
- (4) Kim, H. J.; Paquin, L.; Barney, C. W.; So, S.; Chen, B.; Suo, Z.; Crosby, A. J.; Hayward, R. C. Low-Voltage Reversible Electroadhesion of Ionoelastomer Junctions. *Adv. Mater.* **2020**, *32* (25), 2000600.
- (5) Zhang, C.; Zheng, H.; Sun, J.; Zhou, Y.; Xu, W.; Dai, Y.; Mo, J.; Wang, Z. 3D Printed, Solid-State Conductive Ionoelastomer as a Generic Building Block for Tactile Applications. *Adv. Mater.* **2022**, *34* (2), 2105996.
- (6) Lee, S. W.; Jang, J.; Kim, Y.; Lee, S.; Lee, K.; Han, H.; Lee, H.; Oh, J. W.; Kim, H.; Kim, T.; Dicky, M. D.; Park, C. Intrinsically Stretchable Ionoelastomer Junction Logic Gate Synchronously Deformable with Liquid Metal. *Appl. Phys. Rev.* **2022**, *9* (4), 041404.
- (7) Poh, W. C.; Eh, A. L.-S.; Wu, W.; Guo, X.; Lee, P. S. Rapidly Photocurable Solid-State Poly (Ionic Liquid) Ionogels For Thermally Robust and Flexible Electrochromic Devices. *Adv. Mater.* **2022**, 2206952.
- (8) Gao, D.; Lee, P. S. Rectifying Ionic Current with Ionoelastomers. *Science* **2020**, *367* (6479), 735–736.
- (9) Feng, J.; Wang, Y.; Xu, Y.; Ma, H.; Wang, G.; Ma, P.; Tang, Y.; Yan, X. Construction of Supercapacitor-Based Ionic Diodes with Adjustable Bias Directions by Using Poly(Ionic Liquid) Electrolytes. *Adv. Mater.* **2021**, *33* (31), 2100887.
- (10) Cheng, S.; Chen, B.; Qin, L.; Zhang, Y.; Gao, G.; He, M. Cross-Linked Poly (Ionic Liquid) as Precursors for Nitrogen-Doped Porous Carbons. *RSC Adv.* **2019**, *9* (15), 8137–8145.
- (11) Sha, Y.; Yu, T.; Dong, T.; Wu, X.; Tao, H.; Zhang, H. In Situ Network Electrolyte Based on a Functional Polymerized Ionic Liquid with High Conductivity toward Lithium Metal Batteries. *ACS Appl. Energy Mater.* **2021**, *4* (12), 14755–14765.
- (12) Liang, L.; Chen, X.; Yuan, W.; Chen, H.; Liao, H.; Zhang, Y. Highly Conductive, Flexible, and Nonflammable Double-Network Poly (Ionic Liquid)-Based Ionogel Electrolyte for Flexible Lithium-Ion Batteries. *ACS Appl. Mater. Interfaces* **2021**, *13* (21), 25410–25420.
- (13) Liang, L.; Yuan, W.; Chen, X.; Liao, H. Flexible, Nonflammable, Highly Conductive and High-Safety Double Cross-Linked Poly (Ionic Liquid) as Quasi-Solid Electrolyte for High Performance Lithium-Ion Batteries. *Chem. Eng. J.* **2021**, *421*, 130000.

- (14) Khoo, K. S.; Chia, W. Y.; Wang, K.; Chang, C.-K.; Leong, H. Y.; Maaris, M. N. B.; Show, P. L. Development of Proton-Exchange Membrane Fuel Cell with Ionic Liquid Technology. Sci. Total Environ. 2021, 793, 148705.
- (15) Choi, J.-H.; Xie, W.; Gu, Y.; Frisbie, C. D.; Lodge, T. P. Single Ion Conducting, Polymerized Ionic Liquid Triblock Copolymer Films: High Capacitance Electrolyte Gates for n-Type Transistors. *ACS Appl. Mater. Interfaces* **2015**, *7* (13), 7294–7302.
- (16) Hu, Y.; Teng, Y.; Sun, Y.; Liu, P.; Fu, L.; Yang, L.; Kong, X.-Y.; Zhao, Q.; Jiang, L.; Wen, L. Bioinspired Poly (Ionic Liquid) Membrane for Efficient Salinity Gradient Energy Harvesting: Electrostatic Crosslinking Induced Hierarchical Nanoporous Network. *Nano Energy* 2022, 97, 107170.
- (17) Schroeder, T. B.; Guha, A.; Lamoureux, A.; VanRenterghem, G.; Sept, D.; Shtein, M.; Yang, J.; Mayer, M. An Electric-Eel-Inspired Soft Power Source from Stacked Hydrogels. *Nature* **2017**, *552* (7684), 214–218.
- (18) Huo, R.; Bao, G.; He, Z.; Li, X.; Ma, Z.; Yang, Z.; Moakhar, R.; Jiang, S.; Chung-Tze-Cheong, C.; Nottegar, A. Tough Transient Ionic Junctions Printed with Ionic Microgels. *Adv. Funct. Mater.* **2023**, 2213677.
- (19) Kim, T. Y.; Suh, W.; Jeong, U. Approaches to Deformable Physical Sensors: Electronic versus Iontronic. *Mater. Sci. Eng. R Rep.* **2021**, *146*, 100640.
- (20) Yang, C.; Suo, Z. Hydrogel Ionotronics. *Nat. Rev. Mater.* **2018**, *3* (6), 125–142.
- (21) Dai, S.; Liu, X.; Liu, Y.; Xu, Y.; Zhang, J.; Wu, Y.; Cheng, P.; Xiong, L.; Huang, J. Emerging Iontronic Neural Devices for Neuromorphic Sensory Computing. *Adv. Mater.* **2023**, 2300329.
- (22) Lee, H.-R.; Woo, J.; Han, S. H.; Lim, S.-M.; Lim, S.; Kang, Y.-W.; Song, W. J.; Park, J.-M.; Chung, T. D.; Joo, Y.-C.; Sun, J.-Y. A Stretchable Ionic Diode from Copolyelectrolyte Hydrogels with Methacrylated Polysaccharides. *Adv. Funct. Mater.* **2019**, *29* (4), 1806909.
- (23) Lim, S.-M.; Yoo, H.; Oh, M.-A.; Han, S. H.; Lee, H.-R.; Chung, T. D.; Joo, Y.-C.; Sun, J.-Y. Ion-to-Ion Amplification through an Open-Junction Ionic Diode. *Proc. Natl. Acad. Sci.* **2019**, *116* (28), 13807–13815.
- (24) Gao, D.; Thangavel, G.; Lee, J.; Lv, J.; Li, Y.; Ciou, J.-H.; Xiong, J.; Park, T.; Lee, P. S. A Supramolecular Gel-Elastomer System for Soft Iontronic Adhesives. *Nat. Commun.* **2023**, *14* (1), 1990.
- (25) You, I.; Mackanic, D. G.; Matsuhisa, N.; Kang, J.; Kwon, J.; Beker, L.; Mun, J.; Suh, W.; Kim, T. Y.; Tok, J. B.-H. Artificial Multimodal Receptors Based on Ion Relaxation Dynamics. *Science* 2020, 370 (6519), 961–965.
- (26) Wang, Y.; Wang, Z.; Su, Z.; Cai, S. Stretchable and Transparent Ionic Diode and Logic Gates. *Extreme Mech. Lett.* **2019**, *28*, 81–86.
- (27) Kumar, R.; Mahalik, J. P.; Silmore, K. S.; Wojnarowska, Z.; Erwin, A.; Ankner, J. F.; Sokolov, A. P.; Sumpter, B. G.; Bocharova, V. Capacitance of Thin Films Containing Polymerized Ionic Liquids. *Sci. Adv.* **2020**, *6* (26), eaba7952.
- (28) Shin, S.-J.; Kim, D. H.; Bae, G.; Ringe, S.; Choi, H.; Lim, H.-K.; Choi, C. H.; Kim, H. On the Importance of the Electric Double Layer Structure in Aqueous Electrocatalysis. *Nat. Commun.* **2022**, *13* (1), 174.
- (29) Wu, J. Understanding the Electric Double-Layer Structure, Capacitance, and Charging Dynamics. *Chem. Rev.* **2022**, *122* (12), 10821–10859.
- (30) Bazant, M. Z.; Storey, B. D.; Kornyshev, A. A. Double Layer in Ionic Liquids: Overscreening versus Crowding. *Phys. Rev. Lett.* **2011**, *106* (4), 046102.
- (31) Schmickler, W. Electronic Effects in the Electric Double Layer. *Chem. Rev.* **1996**, *96* (8), 3177–3200.

- (32) Hayes, R.; Warr, G. G.; Atkin, R. Structure and Nanostructure in Ionic Liquids. *Chem. Rev.* **2015**, *115* (13), 6357–6426.
- (33) Fedorov, M. V.; Kornyshev, A. A. Ionic Liquid near a Charged Wall: Structure and Capacitance of Electrical Double Layer. *J. Phys. Chem. B* **2008**, *112* (38), 11868–11872.
- (34) Fedorov, M. V.; Kornyshev, A. A. Ionic Liquids at Electrified Interfaces. *Chem. Rev.* **2014**, *114* (5), 2978–3036.
- (35) Kornyshev, A. A. Double-Layer in Ionic Liquids: Paradigm Change? *The Journal of Physical Chemistry B*, **2007**, *111*, 5545–5557.
- (36) Li, D.-D.; Yang, Y.-R.; Wang, X.-D.; Feng, G. Electrical Double Layer of Linear Tricationic Ionic Liquids at Graphite Electrode. *J. Phys. Chem. C* **2020**, *124* (29), 15723–15729.
- (37) Lockett, V.; Sedev, R.; Ralston, J.; Horne, M.; Rodopoulos, T. Differential Capacitance of the Electrical Double Layer in Imidazolium-Based Ionic Liquids: Influence of Potential, Cation Size, and Temperature. *J. Phys. Chem. C* **2008**, *112* (19), 7486–7495.
- (38) Islam, M. M.; Alam, M. T.; Ohsaka, T. Electrical Double-Layer Structure in Ionic Liquids: A Corroboration of the Theoretical Model by Experimental Results. *J. Phys. Chem. C* **2008**, *112* (42), 16568–16574.
- (39) Alam, M. T.; Islam, M. M.; Okajima, T.; Ohsaka, T. Capacitance Measurements in a Series of Room-Temperature Ionic Liquids at Glassy Carbon and Gold Electrode Interfaces. *J. Phys. Chem. C* **2008**, *112* (42), 16600–16608.
- (40) Liu, X.; Han, Y.; Yan, T. Temperature Effects on the Capacitance of an Imidazolium-Based Ionic Liquid on a Graphite Electrode: A Molecular Dynamics Simulation. *ChemPhysChem* **2014**, *15* (12), 2503–2509.
- (41) Jitvisate, M.; Seddon, J. R. T. Direct Measurement of the Differential Capacitance of Solvent-Free and Dilute Ionic Liquids. *J. Phys. Chem. Lett.* **2018**, *9* (1), 126–131.
- (42) Yu, Z.; Fang, C.; Huang, J.; Sumpter, B. G.; Qiao, R. Molecular Structure and Dynamics of Interfacial Polymerized Ionic Liquids. *J. Phys. Chem. C* **2018**, *122* (39), 22494–22503.
- (43) Kalikin, N. N.; Kolesnikov, A. L.; Budkov, Y. A. Polymerized Ionic Liquids on Charged Electrodes: New Prospects for Electrochemistry. *Curr. Opin. Electrochem.* **2022**, *36*, 101134.
- (44) Budkov, Y. A.; Kalikin, N. N.; Kolesnikov, A. L. Electrochemistry Meets Polymer Physics: Polymerized Ionic Liquids on an Electrified Electrode. *Phys. Chem. Chem. Phys.* **2022**, *24* (3), 1355–1366.
- (45) Armand, M.; Endres, F.; MacFarlane, D. R.; Ohno, H.; Scrosati, B. Ionic-Liquid Materials for the Electrochemical Challenges of the Future. *Nat. Mater.* **2009**, *8* (8), 621–629.
- (46) Kazemiabnavi, S.; Zhang, Z.; Thornton, K.; Banerjee, S. Electrochemical Stability Window of Imidazolium-Based Ionic Liquids as Electrolytes for Lithium Batteries. *J. Phys. Chem. B* **2016**, *120* (25), 5691–5702.
- (47) Tokuda, H.; Tsuzuki, S.; Susan, M. A. B. H.; Hayamizu, K.; Watanabe, M. How Ionic Are Room-Temperature Ionic Liquids? An Indicator of the Physicochemical Properties. *J. Phys. Chem. B* **2006**, *110* (39), 19593–19600.
- (48) Shaplov, A. S.; Vlasov, P. S.; Lozinskaya, E. I.; Ponkratov, D. O.; Malyshkina, I. A.; Vidal, F.; Okatova, O. V.; Pavlov, G. M.; Wandrey, C.; Bhide, A.; Schönhoff, M.; Vygodskii, Y. S. Polymeric Ionic Liquids: Comparison of Polycations and Polyanions. *Macromolecules* **2011**, *44* (24), 9792–9803.
- (49) Dong, J.; Krasnova, L.; Finn, M. G.; Sharpless, K. B. Sulfur (VI) Fluoride Exchange (SuFEx): Another Good Reaction for Click Chemistry. *Angew. Chem. Int. Ed.* **2014**, *53* (36), 9430–9448.

- (50) Lee, O. A.; Ticknor, M.; McBride, M. K.; Hayward, R. C. Pendent Sulfonylimide Ionic Liquid Monomers and Ionoelastomers via SuFEx Click Chemistry. manuscript in preparation (2023).
- (51) Lin, J.; Peng, Z.; Liu, Y.; Ruiz-Zepeda, F.; Ye, R.; Samuel, E. L.; Yacaman, M. J.; Yakobson, B. I.; Tour, J. M. Laser-Induced Porous Graphene Films from Commercial Polymers. *Nat. Commun.* **2014**, *5* (1), 5714.
- (52) Ye, R.; James, D. K.; Tour, J. M. Laser-Induced Graphene. *Acc. Chem. Res.* **2018**, *51* (7), 1609–1620.
- (53) Ye, R.; James, D. K.; Tour, J. M. Laser-Induced Graphene: From Discovery to Translation. *Adv. Mater.* **2019**, *31* (1), 1803621.
- (54) Chen, H.; Choi, J.-H.; Salas-de la Cruz, D.; Winey, K. I.; Elabd, Y. A. Polymerized Ionic Liquids: The Effect of Random Copolymer Composition on Ion Conduction. *Macromolecules* **2009**, *42* (13), 4809–4816.
- (55) Brug, G. J.; van den Eeden, A. L.; Sluyters-Rehbach, M.; Sluyters, J. H. The Analysis of Electrode Impedances Complicated by the Presence of a Constant Phase Element. *J. Electroanal. Chem. Interfacial Electrochem.* **1984**, *176* (1–2), 275–295.
- (56) Vivier, V.; Orazem, M. E. Impedance Analysis of Electrochemical Systems. *Chem. Rev.* **2022**, *122* (12), 11131–11168.

BRIEFS

Table of Contents

